

# Gas-Phase Infrared Photodissociation Spectroscopy of Tetravanadiumoxo and Oxo-Methoxo Cluster Anions

Sandra Feyel,<sup>[b]</sup> Helmut Schwarz,<sup>[b]</sup> Detlef Schröder,<sup>\*[a]</sup> Charles Daniel,<sup>[c]</sup> Hans Hartl,<sup>[c]</sup> Jens Döbler,<sup>[d]</sup> Joachim Sauer,<sup>[d]</sup> Gabriele Santambrogio,<sup>[e]</sup> Ludger Wöste,<sup>[e]</sup> and Knut R. Asmis<sup>[f]</sup>

The infrared spectra of the binary vanadium oxide cluster anions  $V_4O_9^-$  and  $V_4O_{10}^-$  and of the related methoxo clusters  $V_4O_9(OCH_3)^-$  and  $V_4O_8(OCH_3)_2^-$  are recorded in the gas phase by photodissociation of the mass-selected ions using an infrared laser. For the oxide clusters  $V_4O_9^-$  and  $V_4O_{10}^-$ , the bands of the terminal vanadyl oxygen atoms,  $\nu(V-O_v)$ , and of the bridging oxygen atoms,  $\nu(V-O_b-V)$ , are identified clearly. The clusters in which one or two of the oxo groups are replaced by methoxo li-

gands show additional absorptions which are assigned to the C—O stretch,  $\nu(C-O)$ . Density functional calculations are used as a complement for the experimental studies and the interpretation of the infrared spectra. The results depend in an unusual way on the functional employed (BLYP versus B3LYP), which is due to the presence of both  $V-O(CH_3)$  single and  $V=O$  double bonds as terminal bonds and to the strong multireference character of the latter.

## Introduction

Vanadium oxides are increasingly important transition-metal-based catalysts for the oxidative dehydrogenation of propane and in the synthesis of sulfuric acid, maleic anhydride, and phthalic anhydride, among others.<sup>[1]</sup> Nevertheless, systematic development ("catalyst engineering") and improvement of vanadium oxide catalysts is still difficult owing to limited knowledge about mechanistic details of these oxidation reactions, particularly as far as structure-reactivity correlations are concerned. Gas-phase experiments can be employed as a useful and powerful tool to provide complementary insight into the intrinsic structures and binding properties of the transition-metal oxides.<sup>[2]</sup> As far as oxidation of organic compounds is concerned, various types of mass-spectrometric techniques have already been used to investigate the reactions of vanadium oxide ions and their clusters ( $V_mO_n^{+/-}$ ), such as the oxidative dehydrogenation (ODH) of isomeric butenes, small alkanes, and methanol.<sup>[3,4]</sup> With one recent exception,<sup>[5]</sup> the ODH processes are all confined to cationic  $V_mO_n^+$  species, whereas the corresponding anions are much less prone to mediate ODH reactions.

Despite the wealth of new information about the gas-phase chemistry of these ions obtained in reactivity studies, an inherent weakness in this kind of experiment is that usually only the ion mass is observable. In particular, structural features which are of prime interest in transition-metal clusters can often only be accessed indirectly or require the assistance of complementary quantum-chemical studies. Owing to a wealth of energetically low-lying structural and electronic isomers, however, theory alone might encounter difficulties in identifying the lowest energy isomer in transition-metal oxides, not to

mention unambiguously identifying the energetically preferred reaction pathway.<sup>[6]</sup> In fact, it is the combination of the experimentally obtained vibrational spectrum with the calculated frequencies that allows for an unambiguous assignment of the ground-state structure in these systems. In this respect, the availability of powerful infrared lasers in conjunction with recent instrumental developments has opened new prospects

[a] Dr. D. Schröder

Institute of Organic Chemistry and Biochemistry  
Academy of Sciences of the Czech Republic  
Flemingovo nám. 2, 16610 Prague 6 (Czech Republic)  
Fax: (+420) 220-183-583  
E-mail: detlef.schroeder@uochb.cas.cz

[b] S. Feyel, Prof. Dr. H. Schwarz

Institut für Chemie  
Technische Universität Berlin  
Strasse des 17. Juni 135, 10623 Berlin (Germany)

[c] Dr. C. Daniel, Prof. Dr. H. Hartl

Anorganische und Analytische Chemie  
Freie Universität Berlin  
Fabeckstr. 34-36, 14195 Berlin (Germany)

[d] Dr. J. Döbler, Prof. Dr. J. Sauer

Institut für Chemie  
Humboldt Universität Berlin  
Unter den Linden 6, 10099 Berlin (Germany)

[e] G. Santambrogio, Prof. Dr. L. Wöste

Institut für Experimentalphysik  
Freie Universität Berlin  
Arnimallee 14, 14195 Berlin (Germany)

[f] Dr. K. R. Asmis

Fritz-Haber-Institut der Max-Planck-Gesellschaft  
Faradayweg 4-6, 14195 Berlin (Germany)

for the structural characterization of gaseous ions by means of their IR spectra.<sup>[7–9]</sup>

Herein, we combine tandem mass spectrometry with infrared radiation from a free-electron laser to study the IR spectra of the two binary vanadium oxide cluster anions  $V_4O_9^-$  and  $V_4O_{10}^-$  as well as the related methoxy clusters  $V_4O_9(OCH_3)^-$  and  $V_4O_8(OCH_3)_2^-$  for the corresponding mass-selected ions; this approach has already been extensively applied to various pure vanadium oxide ions.<sup>[6, 10, 11]</sup>

## Results and Discussion

As a precursor for the gaseous ions examined in this work by means of their IR spectra, the neutral dodecamethoxy hexavanadiumheptaoxide  $V_6O_7(OCH_3)_{12}$  (**1**, Figure 1) is employed. The infrared spectra of the bulk compound **1** and of some reduced and oxidized derivatives have already been reported.<sup>[12, 13]</sup>

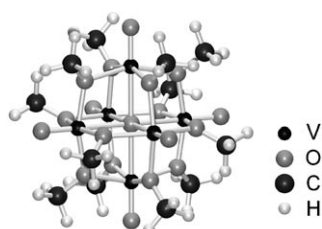


Figure 1. Structure of the neutral precursor **1**.

It was found that the positions of the bands for the bridging oxygen atoms,  $\nu(V-O_b-V)$ , and those of the terminal oxygen atoms of the vanadyl groups,  $\nu(V-O_t)$ , depend on the number of formal  $V^{IV}$  and  $V^V$  centers present, in that both bands show a slight redshift with increasing number of  $V^{IV}$  centers. Instead of counting the number of  $V^{IV}$  and  $V^V$  centers, the formal valence ( $v_f$ ) of vanadium can also be considered. This parameter has the advantage of being independent of cluster size. Within this conceptual framework, each oxygen atom is regarded as a formal  $O^{2-}$  ligand, and a methyl group is treated as formal  $CH_3^+$ , such that the number of oxygen atoms  $N_O$ , the number of methyl groups  $N_{Me}$ , and the single negative charge determine the averaged formal valence of vanadium in the cluster ions as:  $v_f = (2N_O - N_{Me} - 1)/N_V$ , where  $N_V$  stands for the number of vanadium atoms in the cluster. This simple approach often yields non-integer valences, and we explicitly note that 1) the notation neither indicates nor excludes mixed-valence states and 2) the counting scheme can lead to valences larger than  $V^V$  in the case of oxygen-centered radicals, because the formalism treats all oxygen atoms as genuine  $O^{2-}$  ligands, irrespective of the actual bonding situations.

In our ongoing studies on vanadium oxides in oxidation catalysis, we posed the question, whether or not similar trends in the IR frequencies can also be observed for the smaller, gaseous cluster ions that can be produced from the bulk compound  $V_6O_7(OCH_3)_{12}$  via electrospray ionization.<sup>[14]</sup> Herein, we have chosen anionic species, because the cationic vanadium oxide ions show a large tendency for oxidation of attached

methanol or methoxy ligands to formaldehyde concomitant with formation of the corresponding hydroxide clusters. The oxidative dehydrogenation of methanol constitutes a rather interesting topic on its own,<sup>[15–20]</sup> but it is deliberately avoided herein to probe the cluster structures by appropriate spectroscopic means. Specifically, we have investigated the anions  $V_4O_8(OCH_3)_2^-$ ,  $V_4O_9^-$ ,  $V_4O_9(OCH_3)^-$ , and  $V_4O_{10}^-$ , thereby covering a range from  $v_f = 4.25$  in the cases of  $V_4O_8(OCH_3)_2^-$  and  $V_4O_9^-$  through  $v_f = 4.50$  in  $V_4O_9(OCH_3)^-$  to  $v_f = 4.75$  for  $V_4O_{10}^-$ . Furthermore, the pure oxides  $V_4O_9^-$  and  $V_4O_{10}^-$  are regarded as representatives for the vanadia backbone, where the tetravanadium dekaoxide species bears a symmetrical structure similar to  $P_4O_{10}$ ; in comparison, the reduced  $V_4O_9^-$  species lacks one vanadyl oxygen atom. In terms of the formal valence, each consecutive replacement of oxo ligands in  $V_4O_{10}^-$  by methoxy groups in the anions  $V_4O_{10-n}(OCH_3)_n^-$  corresponds to  $\Delta v_f = 0.25$ , thereby relating  $V_4O_8(OCH_3)_2^-$  to  $V_4O_9^-$ , which both have  $v_f = 4.25$ .

Prior to the inspection of the experimental spectra, let us consider the IR bands of major interest expected for these compounds in the range from 500 to 1400  $\text{cm}^{-1}$ , that is, the stretching vibrations of the C–O bonds,  $\nu(C-O)$ , of the terminal oxygen atoms of the vanadyl groups,  $\nu(V-O_t)$ , and the modes characteristic for the bridging oxygen atoms,  $\nu(V-O_b-V)$ . The C–O stretch of free methanol lies at 1027  $\text{cm}^{-1}$  in the gas phase and is found at about 1020  $\text{cm}^{-1}$  in solution.<sup>[21]</sup> For methoxy surface species on vanadia, slightly higher wavenumbers of about 1065  $\text{cm}^{-1}$  have been reported,<sup>[20, 22]</sup> whereas the bridging methoxy ligands of **1** appear at 1031  $\text{cm}^{-1}$ .<sup>[12]</sup> Terminal vanadyl groups have a characteristic band at about 1000  $\text{cm}^{-1}$ , and the bridging oxygen atoms appear in the region somewhat above 600  $\text{cm}^{-1}$ .<sup>[12, 23]</sup>

The ions of interest [ $V_4O_9^-$ ,  $V_4O_{10}^-$ ,  $V_4O_9(OCH_3)^-$ , and  $V_4O_8(OCH_3)_2^-$ ] were prepared via electrospray ionization (ESI), mass-selected, and subsequently irradiated with an IR laser beam while the fragment ions were monitored. Due to the fact that several IR photons are usually required to induce a significant amount of fragmentation, this type of action spectroscopy involves the sequential adsorption of multiple photons. The observed spectral intensities may therefore significantly differ from linear absorption spectra.<sup>[24–26]</sup> Keeping these experimental circumstances in mind, we accordingly focus on the positions of the observed IR bands.

To record the spectra, the major fragmentation pathways of each ion were chosen (Table 1). While in several other systems differences in the IR traces of different fragmentation channels have been observed,<sup>[27]</sup> we found no significant indications for such effects and thus only consider the net photofragmentation yields. For the vanadium oxide anions  $V_4O_9^-$  and  $V_4O_{10}^-$ , loss of neutral  $VO_2$  is observed as, by far, the most prominent fragmentation pathway. In marked contrast, the alkoxo clusters  $V_4O_9(OCH_3)^-$  and  $V_4O_8(OCH_3)_2^-$  exclusively loose neutral  $CH_3$  and thus convert to the binary oxide clusters. This result matches nicely with the previous observation that ESI of  $V_6O_7(OCH_3)_{12}$  under hard conditions can be used for the generation of completely demethylated  $V_mO_n^{+/-}$  cluster ions which have lost all of their alkyl groups.<sup>[14]</sup>

**Table 1.** Mass-selected vanadium oxide cluster anions examined by means of IR spectroscopy in the gas phase along with their major anionic and neutral fragments. Vibrational frequencies derived from the spectra<sup>[a]</sup> are also given.

Parent	Fragments	Position of observed bands [cm <sup>-1</sup> ] <sup>[b]</sup>
V <sub>4</sub> O <sub>9</sub> <sup>-</sup>	V <sub>3</sub> O <sub>7</sub> <sup>-</sup> + VO <sub>2</sub>	634 (m), 715 (w), 780 (w), 990 (s)
V <sub>4</sub> O <sub>10</sub> <sup>-</sup>	V <sub>3</sub> O <sub>8</sub> <sup>-</sup> + VO <sub>2</sub>	633 (m), 998 (s)
V <sub>4</sub> O <sub>9</sub> (OCH <sub>3</sub> ) <sup>-</sup>	V <sub>4</sub> O <sub>10</sub> <sup>-</sup> + CH <sub>3</sub>	624 (s), 999 (s), 1074 (s), 1130 (w), 1155 (w)
V <sub>4</sub> O <sub>8</sub> (OCH <sub>3</sub> ) <sub>2</sub> <sup>-</sup>	V <sub>4</sub> O <sub>10</sub> <sup>-</sup> + 2CH <sub>3</sub>	610 (s), 720 (w), 810 (w), 870 (w), 997 (s), 1065 (s), 1140 (w), 1170 (w)

[a] Positions derived from the peak centers; [b] s=strong, m=medium, w=weak.

### V<sub>4</sub>O<sub>9</sub><sup>-</sup>

The gas-phase IR spectrum of V<sub>4</sub>O<sub>9</sub><sup>-</sup> (Figure 2a), measured by monitoring the VO<sub>2</sub> loss channel (Table 1), is dominated by an intense band centered at 990 cm<sup>-1</sup>. A second, broader feature appears at about 634 cm<sup>-1</sup>, and two weaker features centered at 715 and 780 cm<sup>-1</sup> are observed in between. The intense band is assigned to ν(V–O<sub>t</sub>) of the vanadyl groups, and the feature at 634 cm<sup>-1</sup> coincides with the position expected for the modes of the bridging oxygen atoms, ν(V–O<sub>b</sub>–V). The assignment of the two weaker features remains unclear. One might

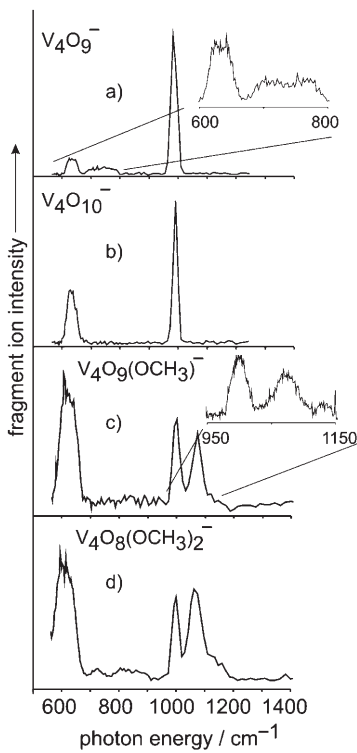


**Figure 2.** Gas-phase IR spectra of a) mass-selected V<sub>4</sub>O<sub>9</sub><sup>-</sup> with an inset showing the expanded range from 600 to 800 cm<sup>-1</sup>, b) mass-selected V<sub>4</sub>O<sub>10</sub><sup>-</sup>, c) mass-selected V<sub>4</sub>O<sub>9</sub>(OCH<sub>3</sub>)<sup>-</sup> with an inset showing the expanded range from 950 to 1050 cm<sup>-1</sup>, and d) mass-selected V<sub>4</sub>O<sub>8</sub>(OCH<sub>3</sub>)<sub>2</sub><sup>-</sup>. The spectra were measured from 550 to 1400 cm<sup>-1</sup> by monitoring the most dominant fragmentation channel. The insets show higher resolution spectra measured with smaller wavelength step sizes, longer dwell times, and in a smaller spectral region.

involve combination bands with low-lying modes of the cluster (computed to lie at about 210 and 360 cm<sup>-1</sup>; see below); similar features are observed in the spectrum of V<sub>4</sub>O<sub>8</sub>(OCH<sub>3</sub>)<sub>2</sub><sup>-</sup>. Consistent with the expected similarities of the ion structures, the gas-phase IR spectrum of V<sub>4</sub>O<sub>9</sub><sup>-</sup> closely resembles that of V<sub>4</sub>O<sub>10</sub><sup>-</sup> (see below).

### V<sub>4</sub>O<sub>10</sub><sup>-</sup>

The gas-phase IR spectrum of V<sub>4</sub>O<sub>10</sub><sup>-</sup> generated by laser vaporization has already been reported,<sup>[28]</sup> and the present results are in good agreement with the previous experimental and theoretical data. According to calculations, a tetragonal D<sub>2d</sub> structure is found for V<sub>4</sub>O<sub>10</sub><sup>-</sup>, which is slightly Jahn–Teller distorted from T<sub>d</sub> symmetry. Each vanadium atom is fourfold coordinated, featuring one V=O bond and three V–O bonds. Assignment of a structure with high symmetry is nicely supported by the simple IR spectrum (Figure 2b) with a dominant narrow signal at about 998 cm<sup>-1</sup> and a weaker, broader signal at 633 cm<sup>-1</sup>; these bands are accordingly assigned to ν(V–O<sub>t</sub>) and ν(V–O<sub>b</sub>–V), respectively. Unlike to V<sub>4</sub>O<sub>9</sub><sup>-</sup>, no indications for combination bands are observed in the spectrum of V<sub>4</sub>O<sub>10</sub><sup>-</sup>, possibly because of the higher symmetry and more stringent selection rules in the latter. Interestingly, the relative intensities of the bands for ν(V–O<sub>t</sub>) and ν(V–O<sub>b</sub>–V) are in better agreement with theory for the present experiment than in previous work.<sup>[28]</sup> Comparison of the results obtained for several V<sub>m</sub>O<sub>n</sub><sup>-</sup> species gives generally good agreement, and the fact that the low-frequency modes are more pronounced in the present study is primarily due to a different optical lens system. The ZnSe window used previously shows a sharp drop in transmission below ca. 650 cm<sup>-1</sup>. Hence, we conclude that the V<sub>m</sub>O<sub>n</sub><sup>-</sup> anions generated in both sources are identical. This result is instructive, because laser vaporization of metals in the presence of O<sub>2</sub> might also give rise to isomeric dioxygen complexes,<sup>[10a,29]</sup> for example V<sub>4</sub>O<sub>8</sub>(O<sub>2</sub>)<sup>-</sup>, which, however, is apparently not the case for the species generated here, as revealed by comparison with the ions obtained via electrospray ionization.

### V<sub>4</sub>O<sub>9</sub>(OCH<sub>3</sub>)<sup>-</sup>

In addition to the vanadyl stretch ν(V–O<sub>t</sub>) at 999 cm<sup>-1</sup>, the gas-phase IR spectrum of the monomethoxo cluster V<sub>4</sub>O<sub>9</sub>(OCH<sub>3</sub>)<sup>-</sup> shows a prominent peak at 1074 cm<sup>-1</sup> with a smaller satellite at about 1130 cm<sup>-1</sup> (Figure 2c). By reference to the infrared data of similar vanadium methoxo species (see above), the more intense of these two latter signals (1074 cm<sup>-1</sup>) is assigned to ν(C–O) and the weaker one near 1130 cm<sup>-1</sup> to a H–C–H bending mode. In the region of the bridging modes ν(V–O<sub>b</sub>–V), a broad signal centered at 624 cm<sup>-1</sup> is observed. Its increased width can be tentatively rationalized by considering the lower symmetry caused by the methoxo ligand, which leads to a splitting of the bridging modes (also see the theoretical results).

$V_4O_8(OCH_3)_2^-$ 

In general, the IR spectrum of  $V_4O_8(OCH_3)_2^-$  (Figure 2d) is similar to that of the monomethoxo cluster. Prominent features appear at 610, 997, and  $1065\text{ cm}^{-1}$ , which are assigned to  $\nu(V-O_b-V)$ ,  $\nu(V-O_t)$ , and  $\nu(C-O)$ , respectively. The major difference in comparison of Figures 2c and d is associated with the increased intensity of the  $\nu(C-O)$  band relative to the other bands, which is consistent with the larger number of C–O oscillators at the expense of free vanadyl groups in the dime-thoxo cluster. In comparison to the pure oxide clusters (Figures 2a and b), the cluster anions containing methoxo ligands (Figures 2c and d) show a much weaker intensity of the  $\nu(V-O_t)$  band than would be expected from the mere consideration of the number of vanadyl moieties replaced by methoxo ligands. Again, weak features are observed between 700 and  $900\text{ cm}^{-1}$  which may be due to combination bands.

### Structural Implications

Even without the consideration of explicitly computed IR spectra, some important structural conclusions can already be drawn from the spectral signatures in Figure 2. At first, the observation of  $\nu(C-O)$  bands in Figures 2c and d indicates the presence of intact methoxy groups in the  $CH_3$ -containing clusters, and thus discounts the occurrence of a possible rearrangement to hydrido species.<sup>[30–32]</sup> Secondly, the increase of the relative intensities of the bands for  $\nu(C-O)$  at the expense of  $\nu(V-O_t)$  indicates that the methoxo ligands replace some of the terminal oxo groups rather than acting as bridging ligands as in the neutral bulk compound 1. The latter view is further supported by the slight blueshift of the  $\nu(C-O)$  bands from  $1031\text{ cm}^{-1}$  in 1 to  $1074\text{ cm}^{-1}$  and  $1065\text{ cm}^{-1}$  in  $V_4O_9(OCH_3)^-$  and  $V_4O_8(OCH_3)_2^-$ , respectively. Hence, the IR spectra reveal structural details which could not have been derived from the mass spectrometric fragmentation patterns alone.

Let us now return to the question posed at the outset of the Results and Discussion and compare the trends observed for the gaseous clusters ions (Table 1) with the IR data reported for the bulk cluster  $V_6O_7(OCH_3)_{12}$  in various redox states. Figure 3 shows plots of the relevant modes  $\nu(V-O_b-V)$  and

$\nu(V-O_t)$  as a function of the formal valence as defined above. The IR frequencies in the gas-phase data (squares) are between 10 and  $40\text{ cm}^{-1}$  higher than those obtained in the condensed phase (circles), which can be accounted for by bulk effects operative in the condensed phase.<sup>[33]</sup> However, the IR spectra of the solid-state clusters show a clear correlation, whereas the trend in the gas-phase data is much less pronounced, if such a correlation exists at all. In Figure 3a, the correlation of the gas-phase data becomes much better if it is assumed that the broad signal at  $634\text{ cm}^{-1}$  for  $V_4O_9^-$  (Figure 2a) comprises two components, the lower of which corresponds to  $\nu(V-O_b-V)$ , which would shift the entry marked with an asterisk closer to the trend observed in the condensed phase (see below).

The above comparison of the infrared bands of vanadium clusters in the condensed phase with the gas-phase data demonstrates that insight into the ion structures is available from the gas-phase infrared spectra even before consideration of theory. Thus, without the information gained from the infrared spectra, the dissociation patterns of the cluster ions, that is, losses of neutral  $VO_2$  from the oxide anions  $V_4O_n^-$  ( $n=9, 10$ ) and losses of methyl groups from  $V_4O_{10-n}(OCH_3)_n^-$  ( $n=1, 2$ ) would have provided almost no structural insight, whereas the IR spectra demonstrate the existence of genuine methoxo ligands in the clusters and also reveal the existence of vanadyl groups and the bridging oxygen atoms. Moreover, the changes in intensities indicate that the methoxo ligands possibly replace the terminal vanadyl groups in the clusters rather than acting as bridging ligands. Even using sophisticated labeling techniques, such a depth of structural information would have been difficult to achieve by mass spectrometry alone, thereby highlighting the additional insight achieved by the combination of mass spectrometric studies with IR radiation from a free electron laser.

### Computational Studies

For a computational prediction or assignment of the IR frequencies, density functional theory is employed. The description of the localization of the d electrons at some of the vanadium sites, that is, the possible existence of mixed-valence structures as opposed to a complete delocalization of the d-

electron density, is known to depend on the amount of Fock exchange in the functional.<sup>[28]</sup> Therefore, the pure generalized gradient functional BLYP and the hybrid functional B3LYP are applied; the latter includes 20% of Fock exchange and is known to favor the localization of electrons.

Figure 4 shows a comparison of the IR bands of the neutral precursor 1 as computed with both methods in the spectral range investigated experimentally, and Table 2 provides a

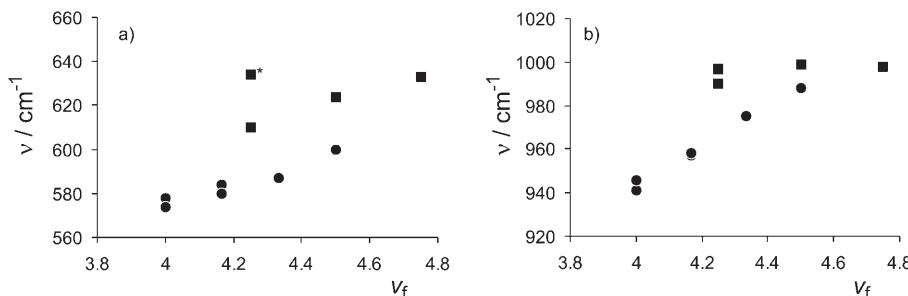


**Figure 3.** Frequencies of a) the modes of the bridging oxygen atoms  $\nu(V-O_b-V)$  in the range from  $570$  to  $640\text{ cm}^{-1}$  and b) the mode of the vanadyl groups  $\nu(V-O_t)$  in the range from  $930$  to  $1010\text{ cm}^{-1}$  as a function of the formal valence ( $v_f$ ) of vanadium in the gaseous clusters studied in this work (■) and in several redox states of the precursor  $V_6O_7(OCH_3)_{12}$  in the solid state (●, data taken from ref. [12]). The asterisk in (a) denotes the peak at  $634\text{ cm}^{-1}$  for  $V_4O_9^-$ ; see text.

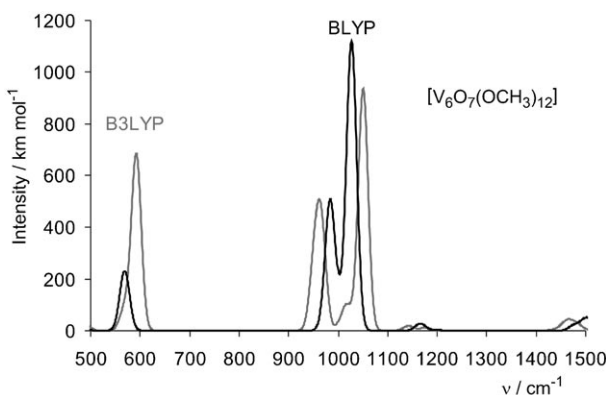


**Figure 4.** Computed IR spectrum of the neutral compound  $V_6O_7(OCH_3)_{12}$  (**1**) in the spectral region probed in the gas-phase experiments with the two different density functionals indicated.

Table 2. Computed band positions ( $\text{cm}^{-1}$ ) of neutral <b>1</b> in the gas phase and the experimentally observed absorptions of <b>1</b> (KBr pellet).			
Mode	BLYP	B3LYP	Experiment
$\nu(V-O_b-V)$	571	594	587
$\nu(V-O_t)$	986	964	975
$\nu(C-O)$	1027	1051	1031

comparison of the calculated band positions with the experimental findings for bulk **1**. Neither of the functionals gives a perfect match with experiment, but the agreement is certainly sufficient given the widths of the IR bands in the experiments. The average deviation for the three modes listed in Table 2 is slightly better for the pure density functional BLYP ( $\pm 10 \text{ cm}^{-1}$ ) than for the hybrid functional B3LYP ( $\pm 13 \text{ cm}^{-1}$ ).

For the scaled frequencies, acceptable agreement with the results of both functionals is also found for the pure vanadium oxide cluster anions  $V_4O_n^-$  with  $n=9$  and 10 (Figures 5a and b). Thus, for  $V_4O_9^-$ , BLYP and B3LYP predict intense bands for  $\nu(V-O_t)$  at  $983 \text{ cm}^{-1}$  and  $960 \text{ cm}^{-1}$ , respectively, and a doublet for the bridging modes  $\nu(V-O_b-V)$  at  $630 \text{ cm}^{-1}$  and  $670 \text{ cm}^{-1}$  for BLYP ( $624 \text{ cm}^{-1}$  and  $645 \text{ cm}^{-1}$  for B3LYP). The computations predict two modes contributing to the experimentally observed

band centered at  $634 \text{ cm}^{-1}$  in the IR spectrum of mass-selected  $V_4O_9^-$  (Figure 2a), which has already been proposed for this particular band on the basis of the experimental spectrum.

Clearly, both BLYP and B3LYP spectra compare reasonably well with the IR spectra for the pure oxide cluster anions.  $V_4O_{10}^-$  has one extra electron in the vanadium d orbitals, and it has already been reported that both functionals predict complete delocalization of this electron.<sup>[28]</sup> Both functionals yield a consistent picture for  $V_4O_9^-$  as well. Two of the three electrons in d orbitals are delocalized in the cluster, and the third electron in the d manifold is localized at the vanadium atom that does not have a terminal oxo ligand. However, pronounced differences between the predictions of the two functionals exist for the anionic cluster ions bearing methoxo ligands  $V_4O_{10-n}(OCH_3)_n^-$  [ $n=1, 2$ ; Figures 5c and d]. While the computed bands for  $\nu(V-O_t)$  and  $\nu(C-O)$  around  $1000 \text{ cm}^{-1}$  still agree reasonably well, the region of the bridging modes is completely different in BLYP and B3LYP, in that the latter functional predicts several modes between  $680$  and  $820 \text{ cm}^{-1}$  that are not found with BLYP and that are also not observed in the experimental gas-phase IR spectra (Figure 2). These differences between BLYP and B3LYP are a consequence of the different degree of localization of the electrons in d states. Whereas

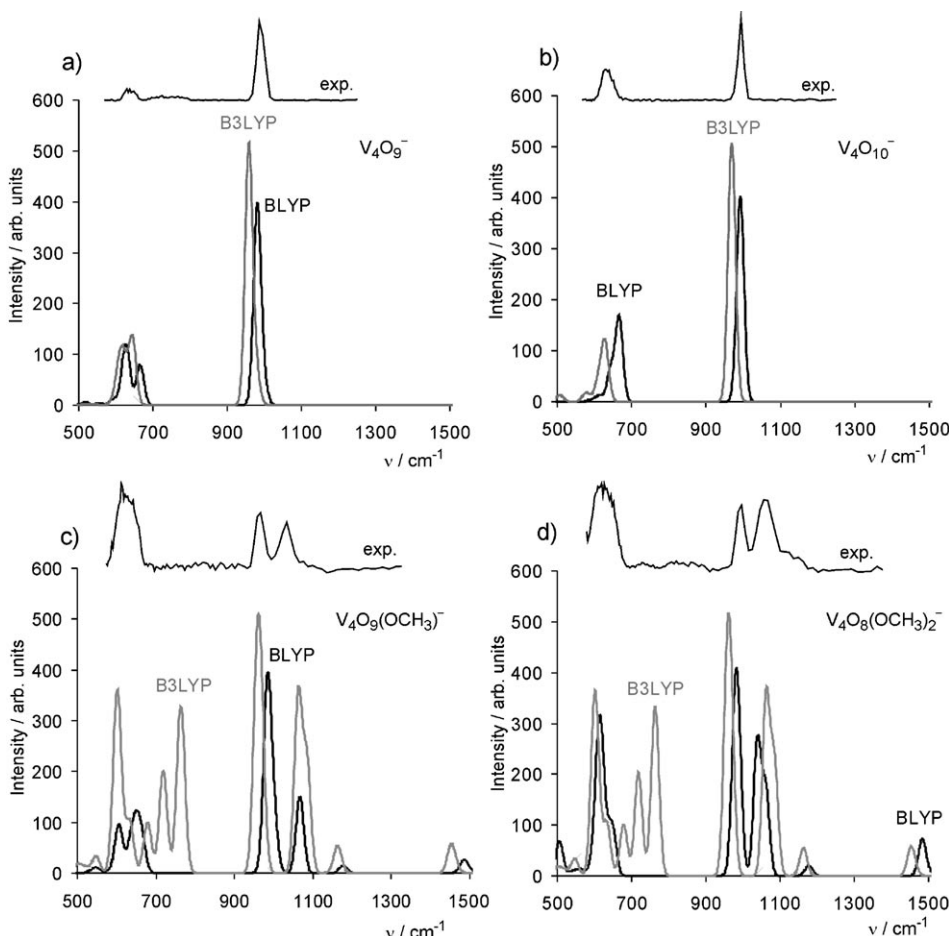


**Figure 5.** Computed IR spectra of the cluster anions a)  $V_4O_9^-$ , b)  $V_4O_{10}^-$ , c)  $V_4O_9(OCH_3)^-$ , and d)  $V_4O_8(OCH_3)_2^-$  using BLYP and B3LYP in the spectral region probed experimentally. For comparison, the corresponding experimental traces are shown above the computed spectra.

BLYP predicts delocalization of the d electrons, B3LYP favors localization of the electrons (two in  $V_4O_9(OCH_3)^-$ , three in  $V_4O_8(OCH_3)_2^-$ ) at the V site(s) with the methoxo ligand(s). The better agreement with the experimental IR spectra indicates that BLYP provides a superior effective description for  $V_{4-10-n}(OCH_3)_n^-$  ( $n=1, 2$ ), that is, for tetrahedral cages having both V=O and V—OCH<sub>3</sub> terminal bonds. The origin of the inferior description of these systems by B3LYP is most likely associated with the pronounced multireference character of the wavefunctions, which is primarily due to the V=O groups.<sup>[34–36]</sup> We note that the treatment of  $V_{4-10-n}(OCH_3)_n^-$  ions and related clusters based on methods using a single determinant obviously is only a first approximation.

Differences between the two functionals also appear in the computed thermochemical data (Table 3). Whereas the C—O

**Table 3.** Selected bond energies (0 K values in eV) of the oxide clusters  $V_4O_9^-$  and  $V_4O_{10}^-$  and the methoxo derivatives  $V_4O_9(OCH_3)^-$  and  $V_4O_8(OCH_3)_2^-$  as well as the calculated C—O bond energy of methoxy radical and dimethyl ether as calculated with BLYP and B3LYP.

Process	$\Delta_r H(\text{BLYP})$	$\Delta_r H(\text{B3LYP})$
$\text{CH}_3\text{O} \rightarrow \text{CH}_3 + \frac{1}{2}\text{O}_2$ <sup>[a]</sup>	1.17	1.24
$\text{CH}_3\text{OCH}_3 \rightarrow \text{CH}_3\text{O} + \text{CH}_3$ <sup>[b]</sup>	3.13	3.14
$V_4O_{10}^- \rightarrow V_4O_9^- + \frac{1}{2}\text{O}_2$	3.84	3.39
$V_4O_9(OCH_3)^- \rightarrow V_4O_{10}^- + \text{CH}_3$	1.07	1.38
$\rightarrow V_4O_9^- + \text{CH}_3\text{O}$	3.74	3.53
$V_4O_8(OCH_3)_2^- \rightarrow V_4O_9(OCH_3)^- + \text{CH}_3$	0.83	1.32
$\rightarrow V_4O_8(OCH_3)^- + \text{CH}_3\text{O}$	3.76	3.58
$\rightarrow V_4O_{10}^- + 2\text{CH}_3$	1.90	2.70
$V_4O_9(OCH_3)^- \rightarrow V_4O_9(\text{H})^- + \text{CH}_2\text{O}$	2.00	2.14

[a] The experimental value is  $(1.33 \pm 0.04)$  eV.<sup>[21]</sup> [b] The experimental value is  $(3.59 \pm 0.04)$  eV.<sup>[21]</sup>

bond dissociation energies of methoxy radical and dimethyl ether are similar with both functionals, only the former is in good agreement with experiment, while that of dimethyl ether is underestimated by both functionals.<sup>[37]</sup> Furthermore, B3LYP appears to favor the oxygen-depleted clusters compared to BLYP, in that the C—O bonds are computed to be stronger with B3LYP, while the V—O bonds to the methoxy groups are weaker with this method. For the loss of two methyl radicals from  $V_4O_8(OCH_3)_2^-$ , that is, the channel used to monitor the gas-phase IR spectrum of this ion, a difference of even 0.80 eV evolves for the two methods.<sup>[38]</sup> Also, the dissociation energy of the V=O bonds in  $V_4O_{10}^-$  is predicted to be lower with B3LYP than with BLYP; from comparison with experiments on  $\text{VO}_2^+$ , we know that B3LYP is closer to the experimental values in this respect.<sup>[38, 39]</sup>

Regardless of the differences between the two functionals, the computed differences of more than 2 eV for the energy demands of CH<sub>3</sub> versus CH<sub>3</sub>O losses are in good agreement with the experimentally observed preference for the former pathway, even in double demethylation. Further, the possible redox processes associated with the oxidation of the methoxo ligand to a formaldehyde molecule were investigated briefly. Even without considering the reaction barrier, both functionals clearly

predict a large preference for the expulsion of a methyl radical from the clusters, which is in perfect match with the experimental data. Last but not least, Figure 6 shows the computed

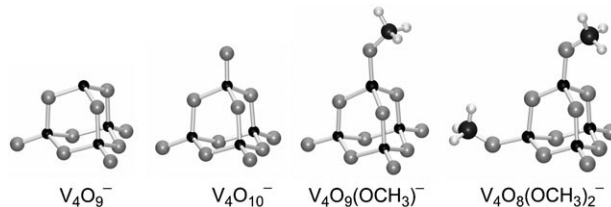


Figure 6. B3LYP structures of  $V_4O_9^-$ ,  $V_4O_{10}^-$ ,  $V_4O_9(OCH_3)^-$ , and  $V_4O_8(OCH_3)_2^-$ .

structures of the four ions under study. We note in passing that for the  $V_{4-10-n}(OCH_3)_n^-$  species, the corresponding structures with bridging methoxo rather than oxo ligands are slightly higher in energy (0.31 eV for  $n=1$  and 0.34 eV for  $n=2$ ). In addition to the higher energy of the structures with bridging methoxy groups, the agreement of the frequencies to the experimental spectra is also worse, as the bridging species bears no C—O stretches in the region of  $1070\text{ cm}^{-1}$ . This finding can be attributed to a weaker C—O bond in bridging coordination due to the threefold coordinated oxygen, which causes a redshift of the C—O stretch into the vanadyl region at about  $1000\text{ cm}^{-1}$ .

## Conclusions

Gas-phase infrared spectra can be used to extract decisive structural information about vanadium oxide and methoxovanadium oxide clusters, even without the explicit consideration of theoretically predicted spectra. In addition to the modes of the bridging and terminal oxo ligands, the methoxovanadium species display characteristic V—OCH<sub>3</sub> stretch modes that are due to the presence of methoxo groups. In general, good agreement is found between the IR spectra of the gaseous ions and the information available for related bulk vanadium clusters. Reasonably good agreement is also found between the experimental infrared spectra and the predictions by the density functional BLYP for all species considered herein; the otherwise powerful B3LYP functional fails for the vibrational spectra of the clusters containing methoxo ligands. The different performance of BLYP and B3LYP for subclasses of vanadium oxide and methoxovanadium oxide clusters with regard to infrared spectra and thermochemical properties shows that there is still room left for developing improved functionals.

## Experimental and Theoretical Methods

The vanadium oxide anions  $V_4O_9^-$  and  $V_4O_{10}^-$  as well as the methoxovanadium oxide clusters  $V_4O_9(OCH_3)^-$  and  $V_4O_8(OCH_3)_2^-$  are studied in the gas phase by infrared spectroscopy. The cluster anions are generated using a guided-ion-beam multipole-based tandem mass spectrometer equipped with an electrospray ionization<sup>[40]</sup> source as described elsewhere.<sup>[10a]</sup> As a precursor for ion generation, the bulk hexanuclear vanadium compound

$V_6O_7(OCH_3)_{12}$  is employed. Similar to the procedure described previously,<sup>[14]</sup> ESI of a methanolic solution of this compound at a flow rate of approximately  $1 \mu\text{L min}^{-1}$  with the source held at ambient temperature and relatively harsh ESI conditions leads to smaller fragment clusters of the general formula  $V_mO_n(OCH_3)_o^-$  ( $m=2-4$ ,  $n=1-11$ ,  $o=0-6$ ). These cluster anions are focused into a radio-frequency (RF) decapole ion guide filled with Ar to collimate the ion beam and compress it in phase space with subsequent  $90^\circ$  deflection into the first RF quadrupole, mass-selection of the ions of interest, and injection using another  $90^\circ$  deflector into a temperature-adjustable, He-filled RF-hexadecapole ion trap.<sup>[10a, 41, 42]</sup> The ion trap is filled continuously for a period of 200 ms and is connected to a helium cryostat ( $T < 16$  K), in which the cluster anions are thermalized by inelastic collisions with the cold buffer gas.

Infrared excitation of the cluster anions is achieved with the free electron laser for infrared experiments (FELIX)<sup>[43]</sup> tuned in a range between 550 and  $1400 \text{ cm}^{-1}$ . Only when in resonance with an allowed IR transition may the cluster anions absorb one or more photons, followed by energy redistribution and subsequent absorption of more photons,<sup>[24]</sup> that is, gradual heating of the ions is achieved. Once a sufficient amount of internal energy is deposited in the ions, they can undergo dissociation to fragment ions of different mass. Directly after the laser pulse, the ions are extracted from the ion trap and the mass-selected ion yields are monitored using the second RF quadrupole mass filter. At each wavelength, the duty cycle is repeated at least ten times such that the acquisition time of a single IR spectrum is on the order of 15 to 30 min; in most cases, several IR spectra are averaged. The laser radiation of FELIX is introduced into the ion trap through a KRS-5 window, a KBr lens of 48 cm focal length, and a 5 mm KBr window. The transmission of this optical setup (ca. 70%) is somewhat lower than that of the previously used ZnSe (up to 85% transmission),<sup>[10a]</sup> but KRS-5 and KBr behave basically wavelength-independent over the 550 to  $1400 \text{ cm}^{-1}$  spectral range investigated herein, whereas the transmission of the ZnSe material is <50% at  $600 \text{ cm}^{-1}$ .

The density functional theory (DFT) calculations are performed with TURBOMOLE 5.8.<sup>[44, 45]</sup> The calculations use the GGA functional BLYP<sup>[46, 47]</sup> as well as the hybrid functional B3LYP.<sup>[47, 48]</sup> In the case of BLYP, the resolution of identity (RI) method<sup>[49, 50]</sup> is used to speed up the calculations. The calculations use the triple-zeta basis sets TZVP of Ahlrichs and co-workers.<sup>[51]</sup> Vibrational spectra were calculated from analytical second derivatives<sup>[52, 53]</sup> using the harmonic approximation. Scaling factors are applied to account for systematic errors of DFT as well as for the neglect of anharmonicities. Because of the multireference character of the V=O bonds, different scaling factors are used for V=O vibrations. Specifically, the scaling factors for the B3LYP frequencies are derived from small  $V_nO_m^+$  ions<sup>[11d]</sup> (0.9171 for  $\nu(V-O)$ ; 0.9832 for all others), and those for BLYP (1.0 for  $\nu(V-O)$ ; 1.0367 for all others) are derived from experimental data for matrix-isolated  $V_4O_{10}^{[54]}$ .

## Acknowledgements

Financial support by the Fonds der Chemischen Industrie and the Deutsche Forschungsgemeinschaft (SFB 546) is gratefully acknowledged. S.F. was supported by a fellowship of the GRK 352. K.R.A., G.S., and S.F. further gratefully acknowledge the support of the Stichting voor Fundamenteel Onderzoek der Materie (FOM) in providing the required beam time on FELIX and highly appreciate the skillful assistance of the FELIX staff. D.S. thanks Otto Dopfer (Berlin) for helpful advice.

**Keywords:** cluster compounds • density functional calculations • IR spectroscopy • polyoxometalates • vanadium

- [1] a) N. Hagen, *Technische Katalyse, Eine Einführung*, Wiley-VCH, Weinheim, 1996; b) G. Centi, F. Cavani, F. Trifirò, *Selective Oxidation by Heterogeneous Catalysis*, Plenum Publishers, New York, 2001.
- [2] Reviews: a) D. Schröder, H. Schwarz, *Angew. Chem.* **1995**, *107*, 2126–2150; *Angew. Chem. Int. Ed.* **1995**, *34*, 1973–1995; b) D. Schröder, S. Shaik, H. Schwarz, *Struct. Bond.* **2000**, *97*, 91–123; c) D. Schröder, H. Schwarz, *Top. Organomet. Chem.* **2007**, *22*, 1–15.
- [3] For examples of oxidation reactions with mononuclear  $VO_n^{+/-}$  species, see: a) J. N. Harvey, M. Diefenbach, D. Schröder, H. Schwarz, *Int. J. Mass Spectrom.* **1999**, *182/183*, 85–97; b) M. Engeser, M. Schlangen, D. Schröder, H. Schwarz, T. Yumura, K. Yoshizawa, *Organometallics* **2003**, *22*, 3933–3943; c) M. Engeser, D. Schröder, H. Schwarz, *Eur. J. Inorg. Chem.* **2007**, 2454–2464.
- [4] For examples of oxidation reactions with  $V_mO_n^{+/-}$  cluster ions, see: a) R. C. Bell, K. A. Zemski, K. P. Kerns, H. T. Denkg, A. W. Castleman, Jr., *J. Phys. Chem. A* **1998**, *102*, 1733–1742; b) R. C. Bell, A. W. Castleman, Jr., *J. Phys. Chem. A* **2002**, *106*, 9893–9899; c) D. R. Justes, R. Mitric, N. A. Moore, V. Bonacic-Koutecky, A. W. Castleman, *J. Am. Chem. Soc.* **2003**, *125*, 6289–6299; d) S. Feyel, D. Schröder, H. Schwarz, *J. Phys. Chem. A* **2006**, *110*, 2647–2654; e) N. A. Moore, R. Mitric, D. R. Justes, V. Bonacic-Koutecky, A. W. Castleman, *J. Phys. Chem. B* **2006**, *110*, 3015–3022; f) S. Feyel, D. Schröder, X. Rozanska, J. Sauer, H. Schwarz, *Angew. Chem.* **2006**, *118*, 4793–4797; *Angew. Chem. Int. Ed.* **2006**, *45*, 4677–4681; g) S. Feyel, J. Döbler, D. Schröder, J. Sauer, H. Schwarz, *Angew. Chem.* **2006**, *118*, 4797–4801; *Angew. Chem. Int. Ed.* **2006**, *45*, 4681–4685.
- [5] T. Waters, G. N. Khairallah, S. A. S. Y. Wimala, Y. C. Ang, R. A. J. O'Hair, A. G. Wedd, *Chem. Commun.* **2006**, 4503–4505.
- [6] K. R. Asmis, J. Sauer, *Mass Spectrom. Rev.* **2007**, *27*, 542–562.
- [7] a) G. v. Helden, I. Hollerman, G. M. H. Knippels, A. F. G. van der Meer, G. Meijer, *Phys. Rev. Lett.* **1997**, *79*, 5234–5237; b) J. Lemaire, P. Boissel, M. Heninger, G. Mauclaire, G. Bellec, H. Mestdagh, A. Simon, S. LeCaer, J. M. Ortega, F. Glotin, P. Maitre, *Phys. Rev. Lett.* **2002**, *89*, 273002.
- [8] J. M. Riveros, in *Encyclopedia of Mass Spectrometry*, Vol. 1, (Ed.: P. B. Armentrout) Elsevier, Amsterdam, **2003**, p. 262–271.
- [9] O. Dopfer, *J. Phys. Org. Chem.* **2006**, *19*, 540–551.
- [10] a) K. R. Asmis, M. Brümmer, C. Kaposta, G. Santambrogio, G. v. Helden, G. Meijer, K. Rademann, L. Wöste, *Phys. Chem. Chem. Phys.* **2002**, *4*, 1101–1104; b) M. Brümmer, C. Kaposta, G. Santambrogio, K. R. Asmis, *J. Chem. Phys.* **2003**, *119*, 12700–12703; c) K. R. Asmis, G. Meijer, M. Brümmer, C. Kaposta, G. Santambrogio, L. Wöste, J. Sauer, *J. Chem. Phys.* **2004**, *120*, 6461–6470.
- [11] See also: a) A. Fielicke, G. Meijer, G. v. Helden, *Europ. Phys. J. D: At. Mol. Opt. Phys.* **2003**, *24*, 69–72; b) A. Fielicke, R. Mitric, G. Meijer, V. Bonacic-Koutecky, G. von Helden, *J. Am. Chem. Soc.* **2003**, *125*, 15716–15717; c) E. Janssesen, G. Santambrogio, M. Brümmer, L. Wöste, P. Lievens, J. Sauer, G. Meijer, K. R. Asmis, *Phys. Rev. Lett.* **2006**, *96*, 233401; d) K. R. Asmis, A. Fielicke, G. v. Helden, G. Meijer, in *The Chemical Physics of Solid Surfaces. Atomic Clusters: From the Gas Phase to Deposited Atomic Clusters*, Vol. 12, (Ed.: D. P. Woodruff) Elsevier, Amsterdam, in press.
- [12] J. Spandl, C. Daniel, I. Brüdgam, H. Hartl, *Angew. Chem.* **2003**, *115*, 1195–1198; *Angew. Chem. Int. Ed.* **2003**, *42*, 1163–1166.
- [13] See also: C. Daniel, H. Hartl, *J. Am. Chem. Soc.* **2005**, *127*, 13978–13987.
- [14] D. Schröder, M. Engeser, M. Brönstrup, C. Daniel, J. Spandl, H. Hartl, *Int. J. Mass Spectrom.* **2003**, *228*, 743–757.
- [15] D. Schröder, J. Loos, M. Engeser, H. Schwarz, C. Jankowiak, R. Berger, R. Thissen, O. Dutuit, J. Döbler, J. Sauer, *Inorg. Chem.* **2004**, *43*, 1976–1985.
- [16] M. Engeser, D. Schröder, H. Schwarz, *Chem. Eur. J.* **2005**, *11*, 5975–5987.
- [17] M. Kaczorowska, D. Schröder, H. Schwarz, *Eur. J. Inorg. Chem.* **2005**, 2919–2923.
- [18] D. Schröder, M. Engeser, H. Schwarz, E. C. E. Rosenthal, J. Döbler, J. Sauer, *Inorg. Chem.* **2006**, *45*, 6235–6245.
- [19] S. Feyel, L. Scharfenberg, C. Daniel, H. Hartl, D. Schröder, H. Schwarz, *J. Phys. Chem. A* **2007**, *111*, 3278–3286.

- [20] J. Döbler, M. Pritzsche, J. Sauer, *J. Am. Chem. Soc.* **2005**, *127*, 10861–10868.
- [21] NIST Standard Reference Database Number 69, Gaithersburg, **2005**, see: <http://webbook.nist.gov/chemistry/>.
- [22] S. Pak, C. E. Smith, M. P. Rosynek, J. H. Lunsford, *J. Catal.* **1997**, *165*, 73–79.
- [23] V. Brazdova, M. V. Ganduglia-Pirovano, J. Sauer, *Phys. Rev. B* **2004**, *69*, 165420.
- [24] a) J. Oomens, A. G. G. M. Tielens, B. G. Sartakov, G. v. Helden, G. Meijer, *Astrophys. J.* **2003**, *591*, 968–985; b) J. Oomens, B. G. Sartakov, G. v. Helden, G. Meijer, *Int. J. Mass Spectrom.* **2006**, *254*, 1–19.
- [25] D. Schröder, H. Schwarz, P. Milko, J. Roithová, *J. Phys. Chem. A* **2006**, *110*, 8346–8353.
- [26] N. C. Polfer, J. Oomens, R. C. Dunbar, *Phys. Chem. Chem. Phys.* **2006**, *8*, 2744–2751.
- [27] J. Oomens, D. T. Moore, G. Meijer, G. v. Helden, *Phys. Chem. Chem. Phys.* **2004**, *6*, 710–718.
- [28] K. R. Asmis, G. Santambrogio, M. Brümmer, J. Sauer, *Angew. Chem.* **2005**, *117*, 3182–3185; *Angew. Chem. Int. Ed.* **2005**, *44*, 3122–3125.
- [29] D. Schröder, P. Jackson, H. Schwarz, *Eur. J. Inorg. Chem.* **2000**, *1171*–1175.
- [30] A. Fiedler, D. Schröder, H. Schwarz, B. L. Tjelta, P. B. Armentrout, *J. Am. Chem. Soc.* **1996**, *118*, 5047–5055.
- [31] G. N. Khairallah, R. A. J. O'Hair, M. I. Bruce, *Dalton Trans.* **2006**, 3699–3707.
- [32] M. Schlangen, H. Schwarz, D. Schröder, *Helv. Chim. Acta* **2007**, *90*, 847–853.
- [33] M. Jacox, *Chem. Soc., Rev.* **2002**, *31*, 108–115.
- [34] While the  $V_4O_{10-n}(OCH_3)_n^-$  systems consist of significantly different building units [ $(O-)_3V=O$  sites with  $V=O$  bonds and tetravalent  $(O-)_3V-OCH_3$  sites in which the  $V=O$  double bond is replaced by a  $V-O$  single bond], comparison of the two functionals yields a different picture when cage-type structures consisting of only  $(O-)_3V=O$  building units are considered. In the series  $V_4O_{10}^-$ ,  $V_6O_{15}^-$ , and  $V_8O_{20}^-$ , a qualitative change of the IR spectra is observed, which is due to a size-dependent localization of the extra electron in  $V_6O_{15}^-$  and  $V_8O_{20}^-$ .<sup>[28]</sup> In this case, electron correlation differences between  $V=O$  double and  $V-O$  single bonds is not an issue, and localization among weakly interacting identical sites depends on a proper self-interaction correction, which is achieved by the Fock exchange in B3LYP, but not in BLYP.
- [35] With single-reference methods, the vanadyl bond length is consistently too short, and consequently the stretching frequency too high. This trend has been found empirically,<sup>[10a]</sup> and we account for it by using a different scaling factor for vanadyl. In a recent study of  $VOF_3$ , it was found that only by using a multireference approach, that is, CASPT2, the vibrational frequency is correctly reproduced (J. Döbler, J. Sauer, unpublished results). The reason for these difficulties are significant charge-transfer interactions of the p orbitals of the vanadyl oxygen atom to vanadium d states.
- [36] For the theoretical challenges arising from an accurate description of  $V-O$  bonds also see: a) C. Rue, P. B. Armentrout, I. Kretzschmar, D. Schröder, J. N. Harvey, H. Schwarz, *J. Chem. Phys.* **1999**, *110*, 7858–7870; b) D. Schröder, M. Engeser, H. Schwarz, J. N. Harvey, *ChemPhysChem* **2002**, *3*, 584–591.
- [37] For an earlier note on this problem, see: D. Schröder, M. C. Holthausen, H. Schwarz, *J. Phys. Chem. B* **2004**, *108*, 14407–14416.
- [38] J. Sauer, J. Döbler, *Dalton Trans.* **2004**, *19*, 3116–3121.
- [39] The computed bond lengths of the methoxy clusters also show differences of up to 0.1 Å between B3LYP and BLYP. A more adequate description would certainly require a multireference approach (also see Ref. [35]).
- [40] J. B. Fenn, *Angew. Chem.* **2003**, *115*, 3999–4024; ..
- [41] G. G. Dolnikowski, M. J. Kristko, C. G. Enke, J. T. Watson, *Int. J. Mass Spectrom. Ion Processes* **1988**, *82*, 1–15.
- [42] J. Westergren, H. Grönbeck, S.-G. Kim, D. Tomanek, *J. Phys. Chem.* **1997**, *107*, 3071–3079.
- [43] D. Oepts, A. F. G. van der Meer, P. W. van Amersfoort, *Infrared Phys. Technol.* **1995**, *36*, 297–308.
- [44] R. Ahlrichs, M. Bär, M. Häser, H. Horn, C. Kölmel, *Chem. Phys. Lett.* **1989**, *162*, 165–169.
- [45] O. Treutler, R. Ahlrichs, *J. Chem. Phys.* **1995**, *102*, 346–354.
- [46] A. D. Becke, *Phys. Rev. A* **1988**, *38*, 3098–3100.
- [47] C. Lee, W. Yang, R. G. Parr, *Phys. Rev. B* **1988**, *37*, 785–789.
- [48] A. D. Becke, *J. Chem. Phys.* **1993**, *98*, 5648–5652.
- [49] K. Eichkorn, O. Treutler, H. Öhm, M. Häser, R. Ahlrichs, *Chem. Phys. Lett.* **1995**, *240*, 283–289.
- [50] K. Eichkorn, F. Weigend, O. Treutler, R. Ahlrichs, *Theor. Chem. Acc.* **1997**, *97*, 119–124.
- [51] A. Schäfer, C. Huber, R. Ahlrichs, *J. Chem. Phys.* **1994**, *100*, 5829–5835.
- [52] P. Deglmann, F. Furche, R. Ahlrichs, *Chem. Phys. Lett.* **2002**, *362*, 511–518.
- [53] P. Deglmann, F. Furche, *J. Chem. Phys.* **2002**, *117*, 9535–9538.
- [54] I. R. Beattie, J. S. Ogden, D. D. Price, *Inorg. Chem.* **1978**, *17*, 3296–3297.

Received: April 16, 2007

Published online on July 2, 2007